JOURNAL OF Materials CHEMISTRY

Effects of metal ions on the morphology and structure of haematite particles produced from forced hydrolysis reaction

Kazuhiko Kandori,* Yasuhito Aoki, Akemi Yasukawa and Tatsuo Ishikawa

School of Chemistry, Osaka University of Education, Asahigaoka 4-698-1, Kashiwara-shi, Osaka 582-8582, Japan. E-mail: kandori@cc.osaka-kyoiku.ac.jp

Received 20th April 1998, Accepted 20th July 1998

The effects of metal ions (Cu^{II}, Ni^{II}, Co^{II} and Cr^{III}) on the morphology and structure of haematite particles, produced from a forced hydrolysis reaction of $FeCl_3$–HCl at various concentrations of metal ions ranging from 0–0.8 in Me/(Fe + Me) atomic ratio (X_{Me}), were investigated by various means. Spherical and a few double-spherical haematite particles were altered to diamond-shaped particles with increase in the concentration of divalent metal ions accompanied by a reduction of particle size up to $X_{Me} = 0.8$. On the other hand, spherical haematite particles with a few double-spherical particles were formed for the system doped with Cr^{III} at $X_{Cr} \leqslant 0.04$ but no pure haematite particle was produced above this concentration. TEM and XRD suggested that the haematite particles formed at $X_{Cu} \leqslant 0.4$ and $X_{Cr} \leqslant 0.04$ are polycrystalline with an enlarged c edge length in the unit cell, though the diamond-like particles produced at $X_{Cu} \geqslant 0.6$ exhibited a single-crystal nature. TG and FTIR indicated that the haematite particles produced with metal ions are hydrohaematite and contain OH^- ions in the lattice. The rate of phase transformation from β-FeOOH to haematite was closely related to the crystal lattice distortion and the amounts of the lattice OH^- ions which affected the morphology and structure of the haematite particles. Part of the dopants were incorporated into the particles and were concentrated in the particle surface phase.

The formation mechanism of monodispersed particles has become an important point that needs to be satisfactorily explained in colloidal systems, although it has empirically been revealed that the preparation of monodispersed particles places severe restriction on various parameters, such as the concentration of reacting components, pH, temperature, mode of mixing, type of vessel employed, *etc.*[1–3] Recently, several investigations have attempted to find answers to this subject employing haematite (α-Fe_2O_3) particles with different morphologies and narrow size distribution, synthesized from a forced hydrolysis reaction of a $FeCl_3$–HCl solution, developed by Matijević *et al.*[1,2,4] It has been revealed that spherical haematite particles were formed *via* a dissolution–recrystallization reaction following the classical La Mer mechanism, while ellipsoidal particles produced with small amounts of phosphate ions are formed through an aggregation process from smaller primary particles.[5–7] Similar aggregation mechanisms were also reported for the formation of cubic particles.[8] However, little is known about the formation process and structural character of these uniform particles except for our studies.[9,10] We revealed previously that the cubic (edge length *ca.* 1.00 μm) and large spherical (diameter *ca.* 0.82 μm) particles are polycrystalline and are constructed by aggregation of fine ferric oxide hydroxide primary particles.[9,10] Recently, we also reported the effect of various types of organic compounds such as amines, dimethylformamide (DMF) and dioxane (DX) on the precipitation of haematite particles and disclosed the structural character of the characteristic haematite particles produced.[11–13] Besides these organic additives, it can be further expected that inorganic metal ions will strongly affect the forced hydrolysis reaction of Fe^{III} in acidic solution on the build-up of polynuclear species from mononuclear iron species and vary the morphology of haematite particles. Metal ions doped into the crystal structure of haematite particles will also offer characteristic valuable properties. Indeed, in the electronic industry, trace amounts of elements (dopants) such as Nb and Ge are incorporated in haematite to improve its semiconductor properties.[14] Dopants are also added to assist the reduction of iron ores.[14] However, there are no comprehensive reports in the literature to address the effects of metal ions on the formation of haematite particles from forced hydrolysis reaction. This work concerns the influence of various types of metal ions on the formation, size, porosity and surface structures of the haematite particles. The results obtained in the present study will contribute to elucidate the formation mechanism of characteristic haematite particles with various morphologies.

Experimental

Preparation procedure of haematite particles

Haematite particles were prepared by a forced hydrolysis of $FeCl_3$–HCl aqueous solutions containing various amounts of metal ions in essentially the same method as employed in previous work.[11–13] A pyrex glass vial containing a 30 cm^3 reaction solution was tightly closed with a Teflon-lined screw cap and heated in a forced conventional air oven at 100 °C for 7 days. The ageing period was varied, if necessary, to follow the formation mechanism of the particles. The relative concentrations of metal ions, Me/(Fe + Me) atomic ratio (denoted as X_{Me}), were varied from 0–0.8. The total concentrations of metal ions and HCl were fixed at 3.12×10^{-2} and 3.20×10^{-3} mol dm^{-3}, respectively. The condition at $X_{Me} = 0$ provides uniform spherical haematite particles.[11–13] Divalent Cu^{II}, Ni^{II}, Co^{II} and trivalent Cr^{III} chloride salts were used as additive metal ions. The precipitates were filtered through a 0.2 μm Millipore filter, rinsed with deionized and distilled water, and dried in an evacuated dryer at room temperature for 16 h. All the chemicals used were guaranteed reagent grade from Wako Pure Chemical Ltd. and were used without further purification.

Characterization of the particles

Transmission electron microscopy (TEM), X-ray powder diffraction (XRD), *in situ* FTIR, X-ray photoelectron spectroscopy (XPS), adsorption experiments of N_2 and H_2O, CHN elemental analysis and electrophoretic mobility measurements were employed to characterize the synthesized haematite particles. The Fe^{III}, Cu^{II} and Cr^{III} concentrations were deter-

mined by inductively coupled plasma spectroscopy (ICP) after dissolving in dilute HCl solution. IR spectra of the particles embedded in KBr pellets (1 mg in 500 mg KBr) were also measured in air using an FTIR spectrometer. Details of the characterization of the particles are given elsewhere.[9–13]

Results and discussion

Particle texture

To investigate the effect of various metal ions on the formation of haematite particles, X_{Me} was varied widely from 2.0×10^{-5} to 0.8. Fig. 1 shows typical TEM micrographs of precipitated particles after ageing for 7 days with various amounts of Cu^{II} and Cr^{III}. Clearly the shape and size of precipitates vary upon changing the concentration of Cu^{II}; large spherical and a few large double-spherical, large spherical and small diamond-like, and small diamond-like haematite particles were produced at $0\leqslant X_{Cu}\leqslant0.2$, $0.4\leqslant X_{Cu}\leqslant0.6$ and $X_{Cu}=0.8$, respectively. It is noteworthy that higher concentrations of divalent metal ions strongly affect the shape and size of haematite particles. A similar morphology change was observed on the addition of other divalent metal ions. Hence the effects of divalent metal ions were thereafter examined using Cu^{II} only. On the other hand, no remarkable morphological change was seen on the system doped with Cr^{III} at $X_{Cr}\leqslant0.04$ leading to large spherical haematite particles with a few double-spherical ones. This concentration region is in the same doping range used for Cu^{II}

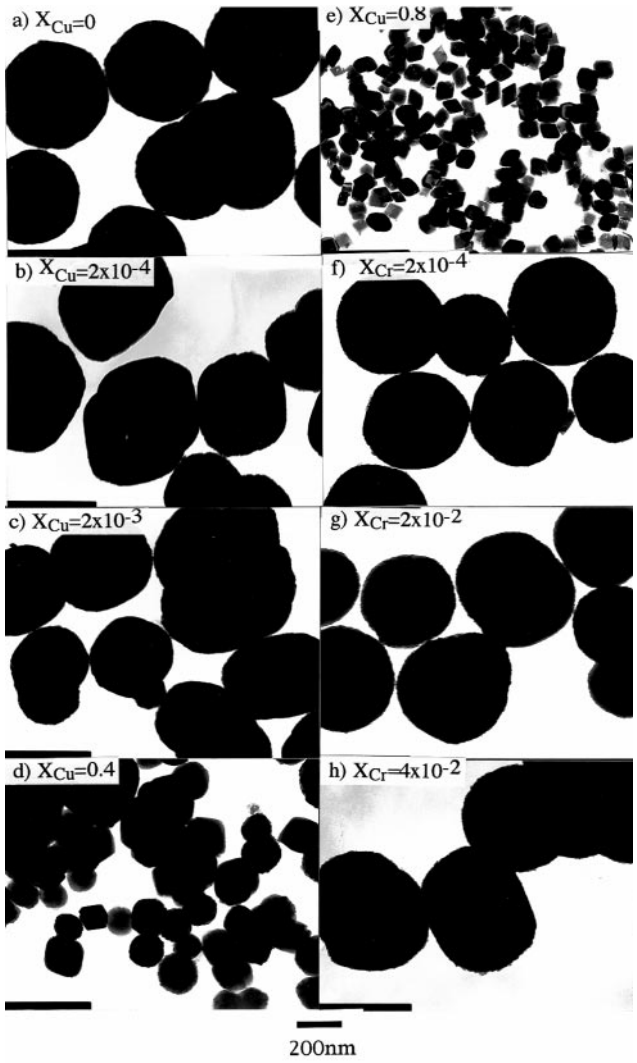

Fig. 1 Typical TEM micrographs of haematite particles produced at various concentrations of Cu^{II} and Cr^{III}.

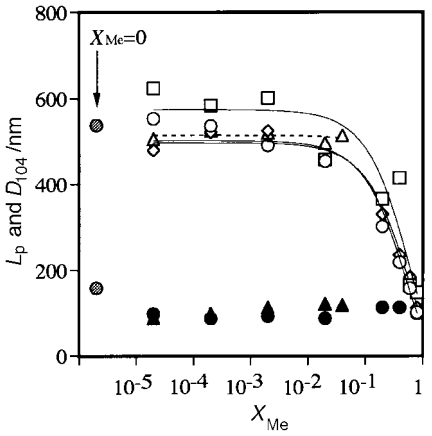

Fig. 2 Changes of mean particle length (L_p) and crystallite sizes from (104) plane (D_{104}) with X_{Me}. L_p: (○) Cu^{II}, (□) Ni^{II}, (◇) Co^{II}, (△) Cr^{II}. D_{104}: (●) Cu^{II}, (▲) Cr^{III}.

ions in which no remarkable change in particle shape and size was observed, which establishes that the effect of doping Cu^{II} and Cr^{III} ions is the same in this region. It should be noted that the haematite formation region of the system doping with Cr^{III} is narrower than those of divalent metal ions. Rod-like β-FeOOH particles were produced together with large spherical haematite particles at $0.05\leqslant X_{Cr}\leqslant0.18$ and no haematite particles precipitated at $X_{Cr}\geqslant0.2$. This result indicates that the inhibitory effect of Cr^{III} ions on the formation of haematite particles is stronger than that for Cu^{II}. Fig. 2 shows the change of mean particle length (L_p) as a function of X_{Me}. The size of the particles produced with divalent metal ions abruptly decreases from *ca.* 500–600 nm to *ca.* 100 nm at $X_{Me}\geqslant0.2$, where the diamond-like haematite particles form, while the L_p of particles precipitated with Cr^{III} remains at *ca.* 500 nm. All of the particles shown in Fig. 1 and 2 exhibit the characteristic XRD pattern of haematite. The crystal structure of haematite was also confirmed by observation of two skeletal vibration bands of haematite at 577 and 483 cm^{-1} in FTIR spectra using KBr disks.

Rate of phase transformation

As confirmed in our previous studies haematite particles are formed by a phase transformation reaction from β-FeOOH to haematite not only in the absence of metal ions but also in the presence of various organic compounds such as amines, DMF and DX[9–13] as already observed by Matijević and Scheiner;[4] β-FeOOH particles precipitated initially are dissolved and recrystallized as haematite. Because the IR bands of β-FeOOH produced with metal ions are weak and broad we monitored the IR band due to haematite in the precipitates formed at various ageing periods over 24 h by the KBr method to reveal the effect of metal ions on this phase transformation reaction. Since the rate of transformation was dramatically varied during the middle of the reaction, we estimated the half-reaction time ($t_{1/2}$) which is required to transforming half of the precipitate into haematite by plotting the relative peak area intensity of the 577 cm^{-1} band due to haematite *vs.* the ageing time. Here the peak area intensity of haematite after ageing for 7 days was taken as 100% in each system. Thus the $t_{1/2}$ value was determined by monitoring the time required to reach 50% of the relative peak area intensity of haematite in each system. The $t_{1/2}$ values evaluated on the systems doped with Cu^{II} and Cr^{III} are plotted as a function of X_{Me} in Fig. 3. A minimum for $t_{1/2}$ occurs for particles produced at $X_{Cu}=2.0\times10^{-4}$ prior to a rapid decrease above $X_{Cu}=0.4$ (open circles). For Cr^{III} doped systems (filled circles), the variation of $t_{1/2}$ is less dramatic than for doping with Cu^{II}, with a minimum occurring at $X_{Cr}=2.0\times10^{-3}$. It is interesting that

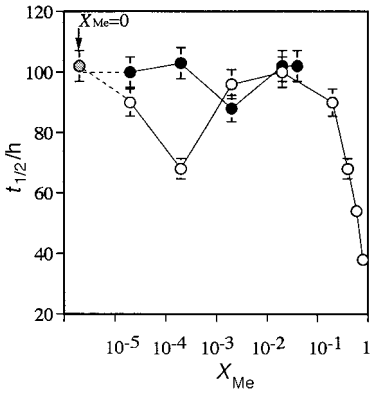

Fig. 3 Changes of half-reaction time of the phase transformation ($t_{1/2}$) with ageing time for the systems doped with Cu^{II} (○) and Cr^{III} (●) ions.

the systems exhibiting slow phase transformation gave large spherical haematite particles with a few double-spherical ones, while the fast phase transformation systems led to small diamond-like particles. This observation is in accord with our previous results using various amines and DMF; acceleration of phase transformation from β-FeOOH to haematite leads to smaller diamond-like single-crystal particles.[12] However, the appearance of minima in the phase transformation reaction at particular concentrations of Cu^{II} and Cr^{III} ions can, as yet, not be explained.

Mechanism of particle formation

It is well known that cationic mononuclear species $Fe(OH)_x(H_2O)_{6-x}^{(3-x)+}$ react with each other to form dinuclear and polynuclear complexes during hydrolysis of Fe^{III}. Simultaneously, decomposition of dinuclear and polynuclear species occurs under acidic conditions, especially at $pH<2$.[15] An extensive study of hydrolysis of Fe^{III} in chloride solution also revealed conspicuous effects of Cl^- on nucleation, growth and aggregation of polynuclear species.[15] The rates of both formation and acid decomposition of polynuclear complexes are considerably enhanced by Cl^-.[15–17] This alteration of the rate of hydrolysis is one of the reasons why the forced hydrolysis reaction of $FeCl_3$–HCl provides various kinds of morphologically characteristic haematite particles. The chemical composition of the polynuclear species, determined by Mössbauer spectra of frozen solutions and X-ray powder patterns of flocculated polynuclear complexes, is polycationic, corresponding to $[FeO_{2/3}(OH)_{4/3}(H_2O)_x]_p^{(p/3)+}$.[15] Hence, it is expected that they coagulate in conjunction with charge compensation by chloride ions, to give species such as $[FeO_{2/3}(OH)_{4/3}(H_2O)_xCl_{1/3}]_p$ $(0.5<x<1.5)$.[15] This fact is supported by the strong effects of Cl^- ions on the morphology of the haematite particles. Recently, Bottero *et al.* also revealed from synchrotron based X-ray spectroscopy that Cl^- ions are incorporated in the structure of iron(III) oxyhydroxides and are easily displaced by OH^-,[18] supporting an interaction between Cl^- ions and particles. During the final precipitation stage, it is plausible to anticipate that aggregation of polynuclear species may involve reversible hydrogen bonding between surface hydroxyl groups. Polynuclear species can be regarded as fine ferric oxide hydroxide primary particles as postulated in our previous work.[9,10]

In the presence of metal ions, it is necessary to take into account the adsorption of metal ions by forming surface complexes with surface hydroxyl groups of polynuclear complexes (PN) involving the coordination of metal ions and release of protons from the surface,[19] *e.g.*, as in eqn. (1)

$$(PN)Fe^{III}\text{–}OH + Cu^{2+} \rightarrow (PN)Fe^{III}\text{–}OCu^{+} + H^{+} \quad (1)$$

There is also a possibility that surface bidentate complexes are formed [eqn. (2)]

$$2(PN\text{–}OH) + Cu^{2+} \rightarrow (PN\text{–}O)_2Cu + 2H^{+} \quad (2)$$

In the presence of trivalent ions, surface hydroxo species can be also formed [eqn. (3)]

$$(PN)Fe^{III}\text{–}OH + Cr^{3+} + H_2O \rightarrow (PN)Fe^{III}\text{–}OCrOH^{+} + 2H^{+} \quad (3)$$

Hence, it is anticipated that dopants may strongly interfere with the aggregation of PNs (primary particles) and produce small diamond-like haematite particles. By contrast, in the presence of high concentrations of metal ions, the enhancement of aggregation of small PN particles may be anticipated by reduction of Coulombic repulsion between charged PN particles. However, L_p dramatically decreases at $X_{Cu} \geqslant 0.2$ (Fig. 2) and this opposite result implies that the inhibitory effect of metal ions for aggregation of PNs by forming surface complexes is dominant over the depression of the electric double layer in bulk solution. Of course, Cr^{III} which has the same valency as Fe^{III} can be incorporated into the haematite particles and this subject will be discussed below. Since the above explanation on the particle formation mechanism can be substantiated by other experiments where β-FeOOH and haematite particles are separately formed, we are currently investigating this subject and a more detailed report will be presented in the future.

Chemical composition

To discuss the effect of metal ions on the particle formation, we assayed the metal contents in the particles [$X_{Me}(P)$] by ICP. Table 1 summarizes $X_{Me}(P)$ of the samples produced at various X_{Me}. Unfortunately, $X_{Me}(P)$ of particles produced at $X_{Cu} \leqslant 2.0\times10^{-2}$ could not be measured since the Cu^{II} content was below the detectable limit of ICP. The $X_{Me}(P)/X_{Me}$ ratio revealed that 0.3–1.2% of Cu^{II} in the starting solution was incorporated into the resulting particles, in contrast to 8–50% of Cr^{III}. This high incorporation of Cr^{III} suggests isomorphous substitution of Cr^{III} for Fe^{III}. The surface atomic ratios [$X_{Me}(S)$] determined by XPS measuring Fe $2p_{3/2}$, Cr $2p_{3/2}$ and Cu $2p_{3/2}$ signals, respectively, at 711.0, 577.4 and 935.9 eV are also listed in Table 1. As expected, $X_{Me}(S)$ rises with an increase in X_{Me} in solutions, although the $X_{Me}(S)$ values of the materials produced at $X_{Cu} \leqslant 0.6$ could not be measured owing to their low content of Cu^{II} in the surface phase. Comparing the ratios of $X_{Me}(S)/X_{Me}(P)$, $X_{Me}(S)$ is 33–1000 times $X_{Me}(P)$, indicating that metal ions are concentrated in the particle surface phase. Given that the documented escaping depths of electrons in XPS of Fe^{III}, Cu^{II} and Cr^{III} ions are 0.78, 0.53 and 0.94 nm,[20] the thickness of these surface phases can be regarded as *ca.* 1 nm. This high surface metal ion content proves the surface complex formation of metal ions with polynuclear surfaces as discussed above [eqn. (1)–(3)].

Crystal structure

The changes of crystallite sizes (denoted as D_{104}) of the particles on doping with Cu^{II} and Cr^{III} estimated by using the Scherrer equation from the half height width of the XRD peaks due to the (104) plane are shown in Fig. 2 by filled circles and filled triangles, respectively. It can be seen that the D_{104} values for both the Cu^{II} and Cr^{III} doped systems are *ca.* 100 nm over the whole range of X_{Me} and are smaller than L_p at $X_{Cu} \leqslant 0.4$ though the D_{104} values of the particles produced at $X_{Cu} \geqslant 0.6$ are compatible with L_p of the corresponding particles. This result implies that the particles produced with Cu^{II} at $X_{Cu} \leqslant 0.4$ and those produced with Cr^{III} are polycrystalline, while the particles formed at $X_{Cu} \geqslant 0.6$ can be regarded as a single-crystals.

To clarify the crystal structure of the particles, unit cell dimensions of the synthetic haematite particles were measured

Table 1 Properties of haematite particles produced with Cu^{II} and Cr^{III}

Me	Me/(Fe+Me) in solution X_{Me}	Shape	Me/(Fe+Me) In particle $X_{Me}(P)$	Me/(Fe+Me) In surface $X_{Me}(S)$	$X_{Me}(P)/X_{Me}$	$X_{Me}(S)/X_{Me}(P)$
Cu	0		0	0	0	0
	2×10^{-5}		—	—	—	—
	2×10^{-4}	Sphere+double sphere	—	—	—	—
	2×10^{-3}		—	—	—	—
	2×10^{-2}		—	—	—	—
	0.2		6.0×10^{-4}	—	3.0×10^{-3}	—
	0.4	Sphere+diamond-like	1.6×10^{-3}	—	4.0×10^{-3}	—
	0.6	Sphere+diamond-like	3.6×10^{-3}	—	6.0×10^{-3}	—
	0.8	Diamond-like	9.3×10^{-3}	0.31	1.2×10^{-2}	33
Cr	2×10^{-5}		—	9.6×10^{-2}	—	—
	2×10^{-4}		1.0×10^{-4}	1.0×10^{-1}	0.50	1000
	2×10^{-3}	Sphere+double sphere	5.0×10^{-4}	1.4×10^{-1}	0.25	280
	2×10^{-2}		2.4×10^{-3}	1.9×10^{-1}	0.12	79
	4×10^{-2}		3.0×10^{-3}	1.9×10^{-1}	0.08	63

with a highly intense X-ray diffractometer source (45 kV, 120 mA). The literature values of the unit cell dimensions of haematite are $a=0.5034$ and $c=1.3752$ nm.[21] Fig. 4 shows a (open symbols) and c unit cell lengths (filled symbols) of the particles as a function of X_{Me} for the systems doped with Cu^{II} and Cr^{III}. The a unit cell lengths of both the systems in Fig. 4 are almost constant at 0.5038 ± 0.0004 nm, corresponding well to the literature unit cell a value while the c unit cell length is much larger than the literature value for haematite and increases with an increase in X_{Me} and then decrease passing through a maximum at $X_{Cu}=2.0\times10^{-4}$ and $X_{Cr}=2.0\times10^{-3}$, respectively. The distortion of the crystal lattice in the c-direction is much more marked for the systems doped with Cu^{II} than with Cr^{III}. This large crystal lattice distortion upon doping with Cu^{II} can be interpreted by a strong Jahn–Teller effect of Cu^{II}; Cu^{II} has a tetragonally distorted coordination sphere in an octahedral coordination. It is interesting that these maxima of c coincide with the minima of $t_{1/2}$ in Fig. 3, indicating that the particles produced with a fast phase transformation rate have an enlarged c unit cell length except for the single-crystal samples produced at $X_{Cu}\geqslant0.6$. Cation substitution in haematite is also reported in the literature.[21] Although the radius of Al^{III} (0.0535 nm) is 17% smaller than Fe^{III} (0.0645 nm), it was reported that up to 1/6 of the Fe positions of haematite produced below 100 °C can be replaced by Al^{III} [22] and can be explained by the isostructural nature of these metal oxides (α-Fe_2O_3 and α-Al_2O_3). On the other hand, Cu^{II} is hardly incorporated into the haematite lattice.[23] This difference is probably due to the strong Jahn-Teller effect of Cu^{II} (0.073 nm) as mentioned above. The unit cell length a linearly decreased with incorporation of Al^{III} whereas c remained essentially invariant. In addition to the difference of ionic radius and valency, the contribution by substituting cations to the crystal field stabilization energy (CFSE) and the change in lattice energy is also proposed to influence the tendency of cations to replace Fe^{III}.[24] The enlarged c unit cell length upon addition of metal ions found in the present study is opposite to results from the literature. Wolska and Schwertmann proposed the enlargement of the c unit cell length of haematite particles by considering the replacement of O^{2-} ions with OH^- ions for an Fe^{3+} deficient species with a general chemical formula α-$Fe_{2-x/3}(OH)_xO_{3-x}$.[25] The lattice OH^- ions contained in haematite particles are necessary to maintain electrical neutrality of Fe^{3+} vacancies and such haematite is termed hydrohaematite. Steinwehr predicted that the crystallographic deviations of oxides produced at low temperature (<100 °C) are attributed to structural imperfections created by the incorporation of OH^- ions into the structure.[26] We also reported that the particles formed with DMF and DX have enlarged c unit cell length and were identified as hydrohaematite.[12,13]

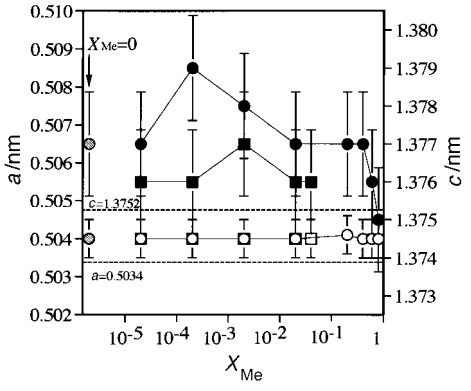

Fig. 4 Changes of unit cell dimensions of haematite particles with X_{Me}. (○, □) a, (●, ■) c; (○, ●) Cu^{II}, (□, ■) Cr^{III}.

IR spectra *in vacuo*

Fig. 5 shows IR spectra in the OH stretching region of the materials pasted on a thin glass plate. These spectra were recorded *in vacuo* at room temperature after evacuation at 100 °C for 2 h and were obtained by subtracting the spectrum

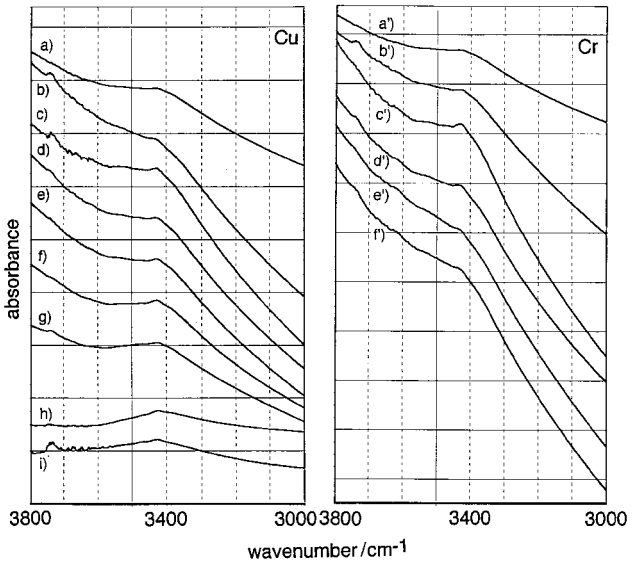

Fig. 5 *In situ* IR spectra of haematite particles produced with various concentrations of Cu^{II} and Cr^{III}. X_{Cu}: (a) 0, (b) 2.0×10^{-5}, (c) 2.0×10^{-4}, (d) 2.0×10^{-3}, (e) 2.0×10^{-2}, (f) 0.2, (g) 0.4, (h) 0.6, (i) 0.8. X_{Cr}: (a′) 0, (b′) 2.0×10^{-5}, (c′) 2.0×10^{-4}, (d′) 2.0×10^{-3}, (e′) 2.0×10^{-2}, (f′) 0.04.

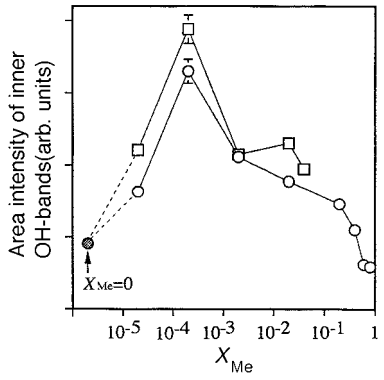

Fig. 6 Changes of the area intensity of inner OH^- band with X_{Me}. (○) Cu^{II}, (□) Cr^{III}.

of the glass plate. An absorption band centered at *ca.* 3400 cm^{-1} was observed for all the materials. We found similar peaks not only on the characteristic haematite particles with spherical, cubic, and diamond-like shapes[9,10] but also on the particles produced with amines,[11] DMF[12] and DX[13] and assigned the band to OH^- ions included in the particles. We can deduce, therefore, that the 3400 cm^{-1} band observed in the present study is derived from the same origin, supporting the existence of lattice OH^- ions in the particles. Fig. 6 compares the area intensity of the lattice OH^- bands of the particles pasted on the glass plate as a function of X_{Me}. It is clear that the amount of OH^- ions incorporated in the lattice of the particles produced with Cu^{II} and Cr^{III} shows maxima at $X_{Cu}=2.0\times10^{-4}$ and $X_{Cr}=2.0\times10^{-4}$. These maxima are fairly in accord with the concentrations of metal ions which exhibit the largest c unit cell length for each system in Fig. 4 ($X_{Cu}=2.0\times10^{-4}$ and $X_{Cr}=2.0\times10^{-3}$), however, the maximum concentration of Cr^{III} in Fig. 6 is shifted to lower concentration by one order of magnitude.

Gas adsorption

Gas adsorption measurement has been addressed in previous work from our laboratory to gain information on the crystallinity and porosity of colloidal particles. Hence, we conducted N_2 and H_2O adsorption experiments on haematite particles by changing the outgassing temperature (OT) of the samples. All the obtained adsorption isotherms were of type II in the IUPAC classification.[26] Then we evaluated the specific surface areas from the adsorption isotherms of N_2 and H_2O, denoted as S_{N_2} and S_{H_2O}, by fitting to the BET equation and using the cross-sectional areas of 0.162 and 0.108 nm^2 of N_2 and H_2O molecules, respectively.[27] The S_{N_2} and S_{H_2O} values of the Cu^{II} and Cr^{III} doped systems are plotted as a function of OT in Fig. 7. The specific surface areas (S_g) of the particles calculated from each particle size using the density of haematite (5.26 g cm^{-3}) are 1–6 m^2 g^{-1}. Clearly, as seen in Fig. 7, S_{N_2} and S_{H_2O} values of all the haematite particles produced with metal ions are much larger than the S_g values, suggesting that these particles are porous. This result strongly implies that the haematite particles examined are constructed by aggregation of polynuclear species as discussed above and underlined in our previous work.[9] Another finding in Fig. 7(A), (A′) is that the S_{N_2} and S_{H_2O} values of the particles produced at $X_{Cu}\leqslant0.4$ vary by elevating the OT (open symbols), but those of the particles formed at $X_{Cu}\geqslant0.6$ show almost constant value (filled symbols), indicating that the crystallinity of the latter particles is higher than that of the former particles. This result indicates that the latter particles have a single-crystal nature as suggested in Fig. 2 and 4. Similar results were also observed on the system doped with Cr^{III} as shown in Fig. 7(B), (B′). However, the variation of S_{N_2} and S_{H_2O} values with OT is less marked than that observed with the Cu^{II} doped system. This result

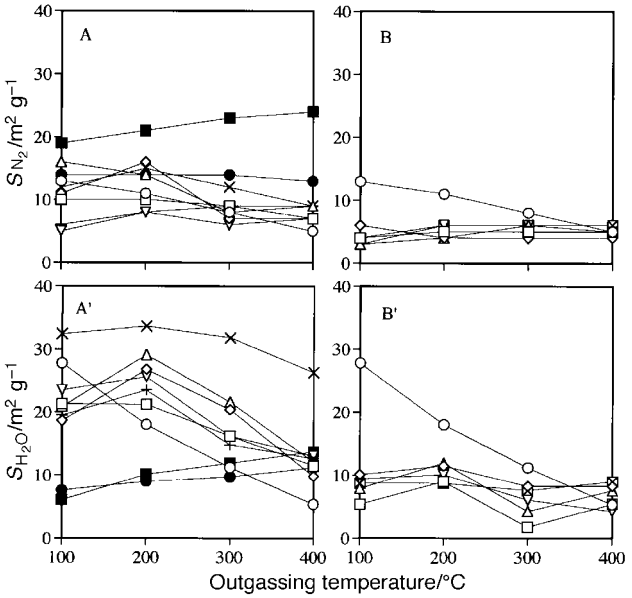

Fig. 7 Change of specific surface areas of the haematite particles produced with various concentrations of Cu^{II} (A, A′) and Cr^{III} ions (B, B′) from nitrogen (S_{N_2}) and water (S_{H_2O}) adsorption experiments as a function of outgassing temperature. (A, A′) X_{Cu}: (○) 0, (□) 2.0×10^{-5}, (◇) 2.0×10^{-4}, (△) 2.0×10^{-3}, (▽) 2.0×10^{-2}, (+) 0.2, (×) 0.4, (●) 0.6, (■) 0.8. (B, B′) X_{Cr}: (○) 0, (□) 2.0×10^{-5}, (◇) 2.0×10^{-4}, (△) 2.0×10^{-3}, (▽) 2.0×10^{-2}, (⊠) 0.04.

indicates that the particles produced with Cr^{III} are more highly crystallized than those precipitated with Cu^{II}, in accord with the results of lattice parameter measurements (Fig. 4).

Fig. 8 shows characteristic t-plots for particles outgassed at 100 °C. The t-plots of all the particles are made up of straight lines passing through the origin at a low pressure branch up to $t=0.3$–0.5 nm but the plots deviate upward above this point by capillary condensation, implying that these particles produce mesopores.[28] The voids between primary particles in the secondary aggregated particles probably constitute a meso-

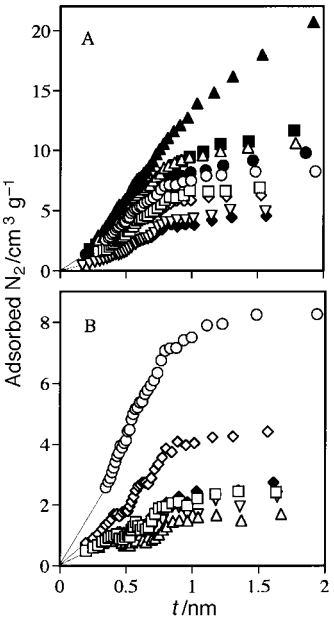

Fig. 8 t-plot curves of haematite particles produced with various concentrations of (A) Cu^{II} and (B) Cr^{III} ions and outgassed at 100 °C. (A) X_{Cu}: (○) 0, (□) 2.0×10^{-5}, (◇) 2.0×10^{-4}, (△) 2.0×10^{-3}, (▽) 2.0×10^{-2}, (◆) 0.2, (●) 0.4, (■) 0.6, (▲) 0.8. (B) X_{Cr}: (○) 0, (□) 2.0×10^{-5}, (◇) 2.0×10^{-4}, (△) 2.0×10^{-3}, (▽) 2.0×10^{-2}, (◆) 0.04.

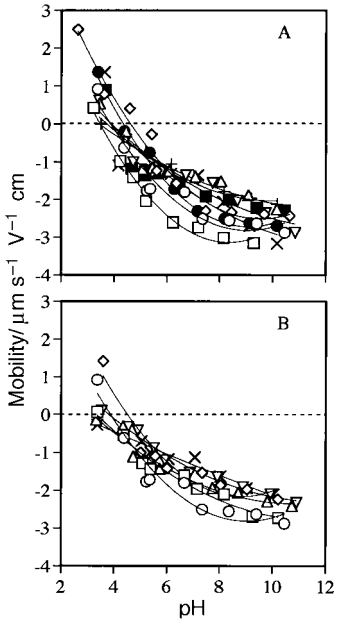

Fig. 9 Changes of the electrophoretic mobility of haematite particles produced with various concentrations of (A) Cu^{II} and (B) Cr^{III} ions. (A) X_{Cu}: (○) 0, (□) 2.0×10^{-5}, (◇) 2.0×10^{-4}, (△) 2.0×10^{-3}, (▽) 2.0×10^{-2}, (×) 0.2, (+) 0.4, (●) 0.6, (■) 0.8. (B) X_{Cr}: (○) 0, (□) 2.0×10^{-5}, (◇) 2.0×10^{-4}, (△) 2.0×10^{-3}, (▽) 2.0×10^{-2}, (×) 0.04.

pore structure, supporting the aggregation mechanism of particle formation.

Surface charge

It can be expected that the accumulation of metal ions in the particle surface phase strongly influences the surface charge. Hence, we measured the electrophoretic mobility of the materials as a function of pH and results are shown in Fig. 9. Particles obtained both with Cu^{II} and Cr^{III} have a lower isoelectric point (iep) than undoped particles ranging from 3.2 to 4.7, indicating that the surface of the particles is strongly acidic. Parks and De Bruyn reported that synthesized Cr_2O_3, $Cu(OH)_2$ and haematite particles have similar iep values of 7.0, 7.6 and 6.7–8.6, respectively.[29] The important role of Cl^- ions by adsorption on the growing particles to induce the surface acidity[13,30] has already been reported, therefore, the actual influence of the metal ions on the iep values of haematite seems to be secondary.

Conclusion

The effects of metal ions on the morphology and texture of haematite particles produced from a forced hydrolysis reaction of a $FeCl_3$–HCl solution were investigated by various means. The morphology and size of the haematite particles varied with increase in the concentration of divalent ions up to $X_{Me}=0.8$, while no remarkable change was observed on doping with Cr^{III} over a narrow concentration region of $X_{Cr}\leqslant0.04$ and no pure haematite particles were precipitated at $X_{Cr}\geqslant0.05$. The particles formed at $X_{Cu}\leqslant0.4$ and $X_{Cr}\leqslant0.04$ are polycrystalline with an enlarged c unit cell length while the particles produced at $X_{Cu}\geqslant0.6$ were single crystals. The change of phase transformation rate from β-FeOOH to haematite by the addition of metal ions was suggested to be closely related to the crystal lattice distortion and amounts of the lattice OH^- ions with various morphologies and structure. Part of the dopant is principally incorporated into the surface of the particles.

We thank Mr. Masao Fukusumi of Osaka Municipal Technical Research Institute for help with the TEM observations. This work has been supported in part by the Grant-in-Aid for Scientific Research (B) from the Ministry of Education, Science, Sports and Culture and Nippon Glass Foundation for Materials Science and Technology, and by The Cosmetology Research Foundation.

References

1 E. Matijević, *Chem. Mater.*, 1993, **5**, 412.
2 E. Matijević, *Annu. Rev. Mater. Sci.*, 1985, **15**, 483.
3 E. K. De Blanco, M. A. Blesa and S. J. Liberman, *React. Solids*, 1986, **1**, 189.
4 E. Matijević and P. Scheiner, *J. Colloid Interface Sci.*, 1978, **63**, 509.
5 M. P. Morales, T. G. Carrero and C. J. Serna, *J. Mater. Res.*, 1992, **7**, 2538.
6 M. Ocana, M. P. Morales and C. J. Serna, *J. Colloid Interface Sci.*, 1995, **171**, 85.
7 M. Ocana, R. R. Clemente and C. J. Serna, *Adv. Mater.*, 1995, **7**, 212.
8 J. K. Bailey, C. J. Brinker and M. L. Mecartney, *J. Colloid Interface Sci.*, 1993, **157**, 1.
9 K. Kandori, Y. Kawashima and T. Ishikawa, *J. Chem. Soc., Faraday Trans.*, 1991, **87**, 2241.
10 K. Kandori, S. Tamura and T. Ishikawa, *Colloid Polym. Sci.*, 1994, **272**, 812.
11 K. Kandori, A. Yasukawa and T. Ishikawa, *J. Colloid Interface Sci.*, 1996, **180**, 446.
12 K. Kandori, N. Okoshi, A. Yasukawa and T. Ishikawa, *J. Mater. Res.*, 1998, **13**, 1698.
13 K. Kandori, Y. Nakamoto, A. Yasukawa and T. Ishikawa, *J. Colloid Interface Sci.*, 1998, **202**, 499.
14 *The Iron Oxides*, *Structure*, *Properties*, *Reaction*, *Occurrence and Uses*, ed. R. M. Cornell and U. Schwertmann, VCH, Weinheim, 1996, p. 38.
15 W. Schneider and B. Schwyn, in *Aquatic Surface Chemistry*, ed. W. Stumm, Wiley-Interscience, New York, 1987, p. 172.
16 W. H. Künzi, dissertation in Eidgenössische Technische Hochschule, Zurich, 1982, No. 7016.
17 W. Schneider, *Comments Inorg. Chem.*, 1984, **3**, 205.
18 J. Bottero, A. Manceau, F. Villieras and D. Tchoubar, *Langmuir*, 1994, **10**, 316.
19 *Chemistry of the Solid–Water Interface*, ed. W. Stumm, Wiley-Interscience, New York, 1992, p. 21.
20 D. R. Penn, *J. Electron Spectrosc.*, 1976, **9**, 29.
21 *Iron Oxides in the Laboratory*, ed. U. Schwertmann and R. M. Cornell, VCH, Weinheim, 1991, p. 10.
22 H. Stanjek and U. Schwertmann, *Clay Clay Miner.*, 1992, **40**, 347.
23 R. M. Cornell and R. Giovannolli, *Polyhedron*, 1988, **7**, 385.
24 B. S. W. Dawson, J. E. Fergusson, A. S. Campbell and E. J. B. Cutler, *Geodarma*, 1985, **35**, 127.
25 E. Wolska and U. Schwertmann, *Z. Kristallogr.*, 1989, **189**, 223.
26 H. E. Steinwehr, *Z. Kristallogr.*, 1967, **125**, 377.
27 K. S. W. Sing, D. M. Everett, R. A. W. Haul, L. Moscou, R. A. Pierotti, J. Rouquerol and T. Siemieniewska, *Pure Appl. Chem.*, 1985, **57**, 603.
28 *Adsorption, Surface Area and Porosity*, ed. S. J. Gregg and K. S. Sing, Academic Press, London, 2nd edn., 1982.
29 G. A. Parks and P. L. de Bruyn, *J. Phys. Chem.*, 1962, **66**, 967.
30 K. Kandori, Y. Kawashima and T. Ishikawa, *J. Colloid Interface Sci.*, 1992, **152**, 284.

Paper 8/02938E